arXiv:1303.7272v1 [cond-mat.quant-gas] 28 Mar 2013

Absence of Bose condensation in certain frustrated lattices

Tigran A. Sedrakyan,[1] Leonid I. Glazman,[2] and Alex Kamenev[1]
[1] William I. Fine Theoretical Physics Institute and Department of Physics,
University of Minnesota, Minneapolis, Minnesota 55455, USA
[2] Department of Physics, Yale University, New Haven, Connecticut 06520, USA
(Dated: April 1, 2013)

We study hard-core bosons on a class of frustrated lattices with the lowest Bloch band having a degenerate minimum along a closed contour in the reciprocal space. We suggest that the ground state of the system is given by non-condensed state, which may be viewed as a state of fermions subject to Chern-Simons gauge field. At fixed density of bosons, such a state exhibits domains of incompressible liquids. Their fixed densities are given by fractions of the reciprocal area enclosed by the minimal energy contour.

There is a recent spike of interest in two dimensional lattices with flat bands both in the context of spin liquids [1–4] and cold atomic gases in optical lattices [5–9]. The archetypical example is a Kagome lattice, where one of the bands (the lowest one for antiferromagnetic sign of hopping integral) is completely non-dispersive[10, 11]. It was shown[12] that below certain critical filling fraction ν_0 (e.g. $\nu_0 = 1/9$ for Kagome lattice) the groundstate of hard core bosons is infinitely compressible. The reason is in the exact degeneracy of non-interacting basis, allowing to form a certain number of non-overlapping localized states. Above the critical concentration the compressibility is finite, but $U(1)$ symmetry remains unbroken signifying the absence of Bose-Einstein condensation (BEC). In the language of spin models, such a groundstate is known as spin-liquid [13–22].

In this letter we show that BEC is absent in a very different family of lattice models. Namely we focus on 2D lattices which lowest energy band exhibits *degenerate minima along a closed contour* in the reciprocal space, Fig. 1. The simplest realizations of this scenario are given by lattices with two cites per unit cell. As an example consider a honeycomb lattice with nearest t_1 and next-nearest t_2 hopping, Fig. 2. The common feature of all such lattices is the Hamiltonian of the form

$$\hat{H} = t_1\hat{T} + t_2\hat{T}^2\,, \qquad \hat{T} = \begin{pmatrix} 0 & \hat{G} \\ \hat{G}^\dagger & 0 \end{pmatrix}, \tag{1}$$

where the matrix structure is in A/B sublattice space and $\hat{G} = G_{\mathbf{k}} = \sum_{j=1,2,3} e^{i\mathbf{k}\cdot\mathbf{e}_j}$ with the three lattice vectors $\mathbf{e}_j$ connecting a site of sublattice A with three nearest neighbors of sublattice B. Three unit vectors $\mathbf{e}_j$ form 120 ° angles with each other, Fig. 2. The Hamiltonians of the form (1) are not limited, though, to the honeycomb lattice. A generic oblique lattice with three distinct nearest and three distinct next-nearest hopping integrals is described by Eq. (1), if *two* conditions are imposed on six hopping constants [23] (variety of other lattices give rise to Hamiltonians of the form (1)).

The two energy bands of the Hamiltonian (1) are given by $E^{(\mp)}_{\mathbf{k}} = \mp|t_1||G_{\mathbf{k}}| + t_2|G_{\mathbf{k}}|^2$. The lowest energy band $E^{(-)}_{\mathbf{k}}$ exhibits a degenerate (flat) minimum along the contour $\mathcal{C}$ in the reciprocal space given by $|G_{\mathbf{k}}| = |t_1|/2t_2$. For the honeycomb lattice this condition[24] is satisfied for $t_2 > |t_1|/6$, Fig. 1. A similar dispersion relation appears in the context of particles with isotropic Rashba spin-orbit coupling [25–30].

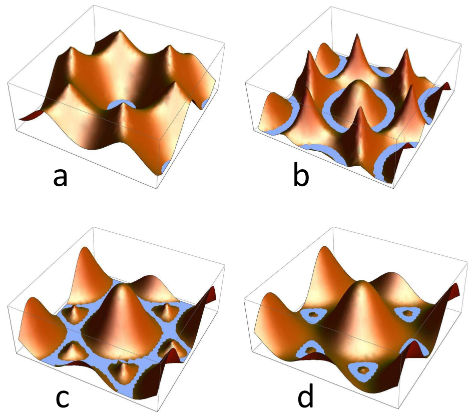

FIG. 1. (Color online) Lowest energy band of the honeycomb lattice with $t_2/t_1 = 0$ (a), 0.3 (b), 0.5 (c), 0.9 (d). The minimal energy contour $\mathcal{C}$ is shown in light gray (blue).

The issue of Bose condensation for particles with such a dispersion relation is a non-trivial one. On the non-interacting level there is no transition at any finite temperature. This is due to the square root, $(E - E_{\mathcal{C}})^{-1/2}$, divergence of the single particle density of states (DOS) near the bottom of the band. Such behavior of DOS highlights similarities with one-dimensional systems, where the groundstate of strongly repulsive bosons is given by the Tonks-Girardeau gas of free fermions [31–35]. Here we show that the effective fermions picture describes the groundstate of hardcore bosons on our 2D lattices as well. The key observation [29] is that the chemical potential of free fermions with the dispersion relation of Fig. 1 scales as $\mu_F \propto \nu^2$ at small enough filling factors ν. This is energetically favorable in comparison with BEC in one of the states along the contour $\mathcal{C}$. The chemical poten-

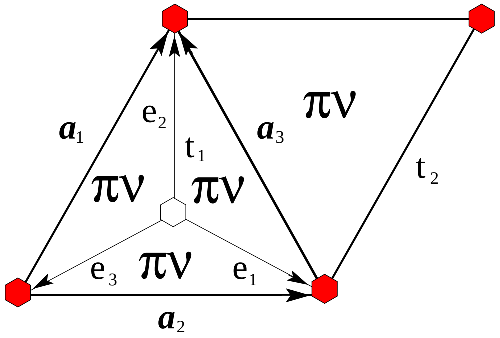

FIG. 2. (Color online) The unit cell of honeycomb lattice with lattice vectors $\boldsymbol{a}_i$ and $\mathbf{e}_i$, $i = 1, 2, 3$. Full (empty) cites belong to the sublattice A (B). Chern-Simons flux through each of the triangles is $\pi\nu$ corresponding to the Haldane modulation of phases with staggered $\phi_H = \Phi/12 = \pi\nu/3$ (see main text).

tial of the latter scales as $\mu_B \propto \nu$. To build a fermionic state of Bose particles one uses Chern-Simons flux attachments familiar in the context of the fractional quantum Hall effect[36–38]. In the mean-field approximation this leads to fermions subject to a uniform magnetic flux $4\pi\nu$ per unit cell superimposed with a particular staggered Haldane[41] flux arrangement. Due to the Pauli principle, the fermions automatically incorporate hard-core condition and thus may be considered as non-interacting. This is the peculiarity of the lattice model with on-site interactions. In a continuum model with spin-orbit interactions, particles with opposite spins still interact[28, 29].

Our main conclusions are as follows: the groundstate energy of hard-core bosons is minimized for a set of *fractionally quantized* filling fractions, determined by the area $\mathcal{A}_\mathcal{C}$ (normalized to a total area of the first Brillouin zone) enclosed by the band minima contour $\mathcal{C}$ in the reciprocal plane[42]

$$\nu_l = \frac{\mathcal{A}_\mathcal{C}}{2l + 1 + \gamma/\pi}\,, \qquad l = 0, 1, \ldots\,, \tag{2}$$

where Berry phase is $\gamma = 0$, if $\mathcal{C}$ encircles the Γ point of the Brillouin zone and $\gamma = \pi$, if $\mathcal{C}$ encircles K and K' points, Fig. 1. States with such filling factors are gapped and incompressible. For density in between the fractionally quantized fillings the system splits into domains with filling factors ν_l and ν_{l+1}. Those states are $U(1)$ symmetric states of composite fermions (CF) occupying the lowest Landau level (or rather the lowest branch of Hofstadter butterfly). The corresponding phase diagram is schematically depicted in Fig. 3.

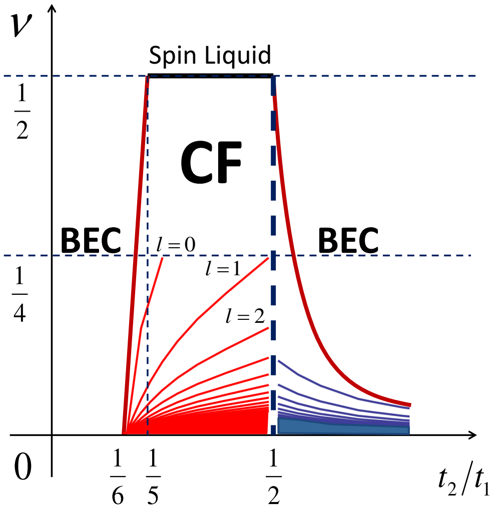

FIG. 3. (Color online) Phase diagram of hard-core bosons on a honeycomb lattice. CF and BEC are composite fermion and Bose condensate states respectively. Also shown incompressible states with fractionally quantized filling fractions ν_l.

Hamiltonian may be written in terms of bosonic creation and annihilation operators $b^\dagger_\mathbf{r}$, $b_\mathbf{r}$, with the hard-core condition $\left(b^\dagger_\mathbf{r}\right)^2 = \left(b_\mathbf{r}\right)^2 = 0$, $\left\{b^\dagger_\mathbf{r}, b_\mathbf{r}\right\} = 1$ (where $\{.,.\}$ denotes anti-commutator), while operators on different sites commute. For, *e.g.*, honeycomb lattice the Hamiltonian takes the form:

$$H = t_1 \sum_{\mathbf{r},j} b^\dagger_\mathbf{r} b_{\mathbf{r}+\mathbf{e}_j} + t_2 \sum_{\mathbf{r},j} b^\dagger_\mathbf{r} b_{\mathbf{r}+\mathbf{a}_j} + H.c. - \mu \sum_\mathbf{r} \left[n_\mathbf{r} - \frac{1}{2} \right], \tag{3}$$

where the vectors $\mathbf{e}_j$ and $\mathbf{a}_j$, $j = 1, 2, 3$ are shown in Fig. 2. Chemical potential, μ, is related to the average on-site occupation ν through an equation of state.

Motivated by the observation that for divergent DOS the fermionic chemical potential is lower than that of the Bose condensate, we proceed with the Chern-Simons transformation[36–40]. To this end we write the bosonic operators as

$$b^{(\dagger)}_\mathbf{r} = c^{(\dagger)}_\mathbf{r}\, e^{\pm i \sum_{\mathbf{r}' \neq \mathbf{r}} \arg[\mathbf{r}-\mathbf{r}'] n_{\mathbf{r}'}}\,, \tag{4}$$

where the summation runs over all sites of the lattice. Since the bosonic operators on different sites commute, the newly defined operators $c_\mathbf{r}$ and $c^\dagger_\mathbf{r}$ obey fermionic commutation relations. Also notice that the number operator is given by $n_\mathbf{r} = c^\dagger_\mathbf{r} c_\mathbf{r}$. Upon transformation (4) hopping terms of the Hamiltonian (3) acquire phase factors $e^{i \sum_{\mathbf{r}''} \phi_{\mathbf{r}'',\mathbf{r}',\mathbf{r}} n_{\mathbf{r}''}}$, where $\phi_{\mathbf{r}'',\mathbf{r}',\mathbf{r}}$ is a scanning angle of the link $\langle \mathbf{r}', \mathbf{r} \rangle$ seen from the lattice site $\mathbf{r}''$. In terms of the fermionic operators the Hamiltonian (3) reads as

$$\begin{aligned} H = t_1 &\sum_{\mathbf{r},j} c^\dagger_\mathbf{r} c_{\mathbf{r}+\mathbf{e_j}} e^{i \sum_{\mathbf{r}'} \phi_{\mathbf{r}',\mathbf{r},\mathbf{r}+\mathbf{e_j}} n_{\mathbf{r}'}} \\ &+ t_2 \sum_{\mathbf{r},j} c^\dagger_\mathbf{r} c_{\mathbf{r}+\mathbf{a_j}} e^{i \sum_{\mathbf{r}'} \phi_{\mathbf{r}',\mathbf{r},\mathbf{r}+\mathbf{a}_j} n_{\mathbf{r}'}} + H.c. \end{aligned} \tag{5}$$

Notice that the hard-core condition is taken care of by the Pauli principle and thus fermions may be considered as non-interacting. A fermion hopping along a closed loop $\mathcal{L}$ on a lattice acquires a phase factor $\prod_{<\mathbf{r}'\mathbf{r}''>\in\mathcal{L}} e^{i\sum_{\mathbf{r}} \phi_{\mathbf{r},\mathbf{r}'\mathbf{r}''} n_{\mathbf{r}}} = \prod_{\mathbf{r}} e^{i\sum_{<\mathbf{r}'\mathbf{r}''>\in\mathcal{L}} \phi_{\mathbf{r},\mathbf{r}'\mathbf{r}''} n_{\mathbf{r}}}$. To analyze the consequences of these factors we adopt the mean-field approximation proven to be effective in the context of the fractional quantum Hall effect [36, 38], $n_{\mathbf{r}} \approx \langle n_{\mathbf{r}}\rangle \equiv \nu$. The phase factor takes the form $e^{i\varphi_{\mathcal{L}}\nu} = \prod_{\mathbf{r}} e^{i\varphi_{\mathbf{r}}\nu}$, where $\varphi_{\mathbf{r}} = \sum_{<\mathbf{r}'\mathbf{r}''>\in\mathcal{L}} \phi_{\mathbf{r},\mathbf{r}'\mathbf{r}''}$ is the total angle obtained by scanning the loop $\mathcal{L}$ from the point $\mathbf{r}$. It is clear that $\varphi_{\mathbf{r}} = 0$ if $\mathbf{r}$ is outside of the loop and $\varphi_{\mathbf{r}} = 2\pi$ if $\mathbf{r}$ is inside. If the reference point $\mathbf{r}$ is exactly on the loop/polygon, $\varphi_{\mathbf{r}}$ is the angle of the polygon corresponding to vertex $\mathbf{r}$. Therefore for a polygon $\mathcal{L}$ with s vertexes enclosing m lattice sites, the phase factor is $\varphi_{\mathcal{L}} = (s-2)\pi + 2\pi m$. This formula has a simple meaning: for *any* triangle (big or small) the flux is $\varphi_{\triangle} = \pi$.

The unit cell of the honeycomb lattice consists of four triangles, Fig. 2, resulting in the average flux $\Phi = 4\pi\nu$ per unit cell. It is clear however that this flux is distributed non uniformly: the half of the unit cell which contains site of sublattice B carries $3\pi\nu$, while the other half $\pi\nu$. There is thus a modulation $\pm\pi\nu$ between the two halves of the unit cell. It is convenient to divide this modulation between the three small triangles, each carrying additional flux $\phi_H = \pi\nu/3 = \Phi/12$. Therefore the *mean-field* treatment of the Chern-Simons phase results in non-interacting fermions subject to a constant magnetic field $\Phi = 4\pi\nu$ *superimposed* with the staggered Haldane phase[41] $\phi_H = \Phi/12$. Below we analyze consequences of this mapping.

We first notice that the flux attachment described above preserves the special form of the Hamiltonian (1) $\hat{H} = t_1\hat{T} + t_2\hat{T}^2$, where $\hat{T}$ is the operator acting in the space $(c^A_{\mathbf{r}}, c^B_{\mathbf{r}})$ and $\hat{G} = \sum_j e^{i\mathbf{e}_j\cdot(\mathbf{k}+\mathbf{A}_{\mathbf{r}})}$, where $\mathbf{A}_{\mathbf{r}}$ is the vector potential of the average magnetic field with $\Phi = 4\pi\nu$ flux per unit cell. Notice that in the presence of the vector potential operators $\hat{G}$ and $\hat{G}^\dagger$ do not commute. Employing Baker-Campbell-Hausdorff[43] formula, one finds $\hat{G}\hat{G}^\dagger = \sum_j e^{i\mathbf{a}_j\cdot(\mathbf{k}+\mathbf{A}_{\mathbf{r}})+i\eta_j\phi_H} + H.c.$ where $-\eta_1 = \eta_2 = \eta_3 = 1$ and $\phi_H = \Phi/12$. This is exactly the next-nearest neighbor hopping over sublattice A in presence of the constant magnetic field *and* Haldane modulation ϕ_H. Similarly $\hat{G}^\dagger\hat{G} = \sum_j e^{i\mathbf{a}_j\cdot(\mathbf{k}+\mathbf{A}_{\mathbf{r}})-i\eta_j\phi_H} + H.c.$ is the hopping along sublattice B in the same setup. Therefore the Haldane modulation, naturally appearing from the mean-field treatment of the Chern-Simons field, is necessary to preserve the form (1) of the Hamiltonian (a constant magnetic field without the modulation does *not* admit representation (1)).

This observation greatly simplifies finding the spectrum by reducing the problem to diagonalization of the operator $\hat{T}$. We first analyze it in the semiclassical approximation, applicable if the minimal energy contour $\mathcal{C}$ encloses relatively small fraction of the Brillouin zone. To this end we notice that the spectrum of the operator $\hat{G} = G_{\mathbf{k}+\mathbf{A}}$ in Eq. (1) can be found using Onsager's relation[44] for Bohr-Sommerfeld quantization of quasiclassical cyclotron orbits in a magnetic field. Denote by $G_l(\Phi)$, $l = 1, 2, \ldots$, the eigenvalues of $G_{\mathbf{k}+\mathbf{A}}$. Semiclassically $G_l(\Phi)$ can be found by: (i) considering the constant energy contours $|G_{\mathbf{k}}| = G$ of the bare operator in the reciprocal $\mathbf{k}$ space, and (ii) identifying $G_l(\Phi)$ with energy of contours $\mathcal{C}_l$ having a normalized reciprocal area $\mathcal{A}(\mathcal{C}_l)$ given by:

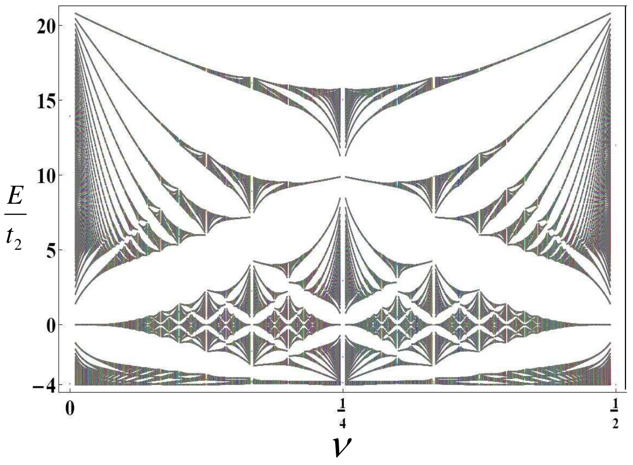

FIG. 4. Hofstadter energy spectrum vs. filling fraction $\nu \in [0, 1/2]$, for $t_2 = t_1/4$, *i.e.* $\mathcal{C}$ is around the Γ point. Notice that the bottom of the Hofstadter spectrum is flat, which is a consequence of the fact that all Landau levels, (8), exhibit minima at the same energy $E = -t_1^2/4t_2$.

$$\mathcal{A}(\mathcal{C}_l) = \left(l + \frac{1}{2} - \frac{\gamma}{2\pi}\right)\frac{\Phi}{2\pi}\,, \tag{6}$$

where Φ is a magnetic flux through a unit cell of the lattice, and γ is the Berry phase[45, 46]. Finally, the spectrum of the Hamiltonian (1), which describes the lattice subject to the constant magnetic flux Φ *and* Haldane modulation $\phi_H = \Phi/12$, is found in terms of $G_l(\Phi)$ as

$$E_l(\Phi) = -t_1 G_l(\Phi) + t_2\big[G_l(\Phi)\big]^2\,. \tag{7}$$

Landau levels (7) are non-monotonic functions of flux, see inset in Fig. 5. They all (apart from $l = 0$ if $\gamma = \pi$) reach the minimum at $G = t_1/2t_2$, i.e. exactly at the band minimum, where the corresponding cyclotron orbit coincides with the minimal energy contour $\mathcal{C}$. Recalling that $\Phi = 4\pi\nu$, one obtains the set of the filling factors ν_l, Eq. (2), where the Landau levels reach the minimum. Since the Chern-Simons transformation (4) attaches exactly one flux quantum per particle, fermions $c_{\mathbf{r}}$ fully fill the lowest Landau level (LLL) at any lattice filling ν. Therefore in the mean-filed approximation the *many-body* groundstate energy follows LLL.

As two examples we consider the cases where $\mathcal{C}$ is close to the Γ point, i.e. $t_2 \gtrsim t_1/6$, and $\mathcal{C}$ is close to K and K', i.e. $t_2 \gg t_1/2$. In the first case, expanding near $\mathbf{k} = 0$, we find $|G_{\mathbf{k}}|^2 \approx 9(1 - k^2/2)$

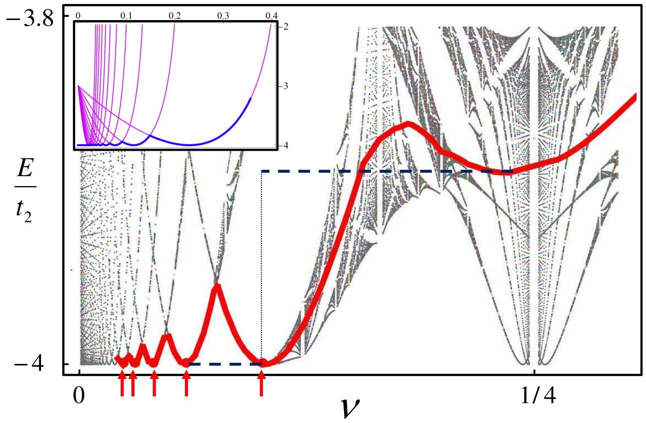

FIG. 5. (Color online) Bottom part of Fig. 4. Thick (red) line represents the ground state energy per particle obtained numerically from the Hofstadter energy spectrum, Eq. (10). Arrows show fractionally quantized filling fractions (2). Dashed line is the microscopic chemical potential exhibiting jumps at the fractionally quantized filling fractions. Inset: Semiclassical Landau levels (8) as functions of the filling fraction ν.

(where $1/k$ is measured in units of lattice spacing), resulting in the constant energy contours with the normalized area $\mathcal{A}(\mathcal{C}_l) = \left(3\sqrt{3}/4\pi\right)(1 - G_l^2/9)$. Taking into account quantization Eq. (6) with $\gamma = 0$, we obtain $G_l = \pm\sqrt{9 - 2\sqrt{3}\Phi(l + 1/2)}$ and

$$E_l^\Gamma(\Phi) = -t_1\sqrt{9 - 2\sqrt{3}\Phi(l + 1/2)} + t_2(9 - 2\sqrt{3}\Phi(l + 1/2)). \tag{8}$$

This semiclassical spectrum is shown in the inset in Fig. 5. In the second case, expanding around K point we find $G_\mathbf{k} \approx 3|k|/2$ and $\gamma = \pi$[41], leading to

$$E_l^K(\Phi) = -t_1\sqrt{\sqrt{3}\Phi l} + t_2\sqrt{3}\Phi l\,. \tag{9}$$

To go beyond the semiclassical approximation we consider the Hofstadter problem on the lattice, including Haldane modulation. For a rational flux $\Phi = 4\pi p/q$ (p and q are positive integers) diagonalization of the operator $\hat{T}$ reduces to Harper equation, which can be analyzed numerically. For such fluxes the spectrum splits onto q non-overlapping subbands, labeled by $m = 1, 2, \ldots q$. The corresponding spectrum $E_{m,\mathbf{k}}(\Phi)$, Fig. 4, acquires the form of the Hofstadter butterfly[47]. Notice the flatness of the lower edge of the spectrum, which reflects the divergent DOS at this energy. Figure 5 amplifies the lowest part of the Hofstadter spectrum. Landau levels, closely following Eq. (8), are visible at small filling fractions.

The mean-field Chern-Simons treatment maps the Hamiltonian (3) onto the system of non-interacting fermions in the Hofstadter spectrum. Since fermions have filling factor $\nu = p/q$, the many-body groundstate is given by occupying p (out of q) lowest subbands. The ground state energy per particle is given by

$$E_{GS}(\nu) = \frac{q}{Np}\sum_{m=1}^{p}\sum_{\mathbf{k}}^{N/q} E_{m,\mathbf{k}}(4\pi p/q)\,, \tag{10}$$

where N is number of lattice sites. In Fig. 5 we show groundstate energy calculated this way vs. filling fraction. For small filling fractions it closely follows the semiclassical lowest Landau levels (8), exhibiting the minima at the fractionally quantized filling fractions ν_l, Eq. (2). This leads to a macroscopic chemical potential, exhibiting staircase shape with the jumps at the fractionally quantized filling fractions (2), see Fig. 5. The flat regions of the staircase imply phase separation into domains with fillings ν_l and ν_{l+1}.

There is direct mapping between the considered hardcore boson system Eq. (3) and XY lattice spin model. Indeed, one may express bosonic creation and annihilation operators $b_\mathbf{r}^{(\dagger)}$ in terms of on-site spin 1/2 operators $b_\mathbf{r}^{(\dagger)} \to \sigma_\mathbf{r}^\mp$ and $(2n_\mathbf{r} - 1) \to \sigma_\mathbf{r}^z$, where $n_\mathbf{r} = b_\mathbf{r}^+ b_\mathbf{r}$ is the on-site density operator. Then the Hamiltonian Eq. (3) acquires the form

$$H = t_1\sum_{\mathbf{r},j}\sigma_\mathbf{r}^+\sigma_{\mathbf{r}+\mathbf{e}_j}^- + t_2\sum_{\mathbf{r},j}\sigma_\mathbf{r}^+\sigma_{\mathbf{r}+\mathbf{a}_j}^- + H.c. - h\sum_\mathbf{r}\sigma_\mathbf{r}^z\,. \tag{11}$$

The z-magnetic field plays the role of the chemical potential $\mu = 2h$, which is related to the average magnetization $m = \nu - 1/2$ through the equation of state $\mu(\nu)$. In this way, BEC state with broken $U(1)$ symmetry translates into magnetically ordered state, while $U(1)$ symmetric CF state is interpreted as spin-liquid. Comparison of CF groundstate energy, Eq. (10), with the energy of the magnetically ordered state of the *classical* spin model[48, 49] shows that at $\nu = 1/2$ (i.e. no magnetic field) the former wins for $1/5 < t_2/t_1 < 1/2$. This suggests the *spin liquid* ground state, Fig. 3, of the corresponding XY spin model, corroborating with recent simulations[18, 50, 51].

We are grateful to O. Starykh and V. Galitski for useful discussions. This work was supported by DOE contract DE-FG02-08ER46482.

[1] L. Balents, Nature (London) **464**, 199 (2010).

[2] S. V. Isakov, M. B. Hastings, and R. G. Melko, Nature Phys. **7**, 772 (2011).

[3] X. Hu, M. Kargarian, and G. A. Fiete, Phys. Rev. B **84**, 155116 (2011).

[4] Y.-F. Wang, H. Yao, Z.-C. Gu, C.-D. Gong, and D. N. Sheng, Phys. Rev. Lett. **108**, 126805 (2012).

[5] C. Wu, D. Bergman, L. Balents, and S. Das Sarma, Phys. Rev. Lett. **99**, 070401 (2007).

[6] C. Wu and S. Das Sarma, Phys. Rev. B **77**, 235107 (2008).

[7] V. Apaja, M. Hyrkäs, and M. Manninen, Phys. Rev. A **82**, 041402(R) (2010).

[8] G.-B. Jo, J. Guzman, C. K. Thomas, P. Hosur, A. Vishwanath, and D. M. Stamper-Kurn, Phys. Rev. Lett. **108**, 045305 (2012).

[9] S. K. Baur and N. R. Cooper, Phys. Rev. Lett. **109**, 265301 (2012).

[10] M. E. Zhitomirsky and H. Tsunetsugu, Phys. Rev. B **70**, 100403(R) (2004).

[11] D. L. Bergman, C. Wu, and L. Balents, Phys. Rev. B **78**, 125104 (2008).

[12] S. D. Huber and E. Altman, Phys. Rev. B **82**, 184502 (2010).

[13] X.-G. Wen, Phys. Rev. B **65**, 165113 (2002).

[14] A. Paramekanti, L. Balents, and M. P. A. Fisher, Phys. Rev. B **66**, 054526 (2002).

[15] P. Phillips and D. Dalidovich, Science **302**, 243 (2003).

[16] S. Yan, D. A. Huse, and S. R. White, Science **332**, 1173 (2011).

[17] D. N. Sheng, O. I. Motrunich, and M. P. A. Fisher, Phys. Rev. B **79**, 205112 (2009).

[18] C. N. Varney, K. Sun, V. Galitski, and M. Rigol, Phys. Rev. Lett. **107**, 077201 (2011).

[19] H.-C. Jiang, H. Yao, and L. Balents, Phys. Rev. B **86**, 024424 (2012).

[20] H. Yao and S. A. Kivelson, Phys. Rev. Lett. **108**, 247206 (2012).

[21] E. Tang, M. P. A. Fisher, and P. A. Lee, Phys. Rev. B **87**, 045119 (2013).

[22] R Chen, H. Ju, H.-C. Jiang, O. A. Starykh, and L. Balents, arXiv:1211.1676.

[23] For three distinct t_1, t_1', t_1'' and t_2, t_2', t_2'' the Hamiltonian has the structure of (1), if $t_1 t_2 = t_1' t_2' = t_1'' t_2''$.

[24] The antiferromagnetic sign $t_2 > 0$, assumed here, implies gauge flux π per triangle (i.e. 2π per unit cell) for bosons on the lattice.

[25] Y. A. Bychkov and E. I. Rashba, J. Phys. C **17** , 6039 (1984).

[26] E. G. Mishchenko, A. V. Shytov, and B. I. Halperin, Phys. Rev. Lett. **93**, 226602 (2004).

[27] D. L. Campbell, G. Juzeliünas, and I. B. Spielman, Phys. Rev. A **84**, 025602 (2011).

[28] E. Berg, M. S. Rudner and S. Kivelson, Phys. Rev. B **85**, 035116 (2012).

[29] T. A. Sedrakyan, A. Kamenev, and L. I. Glazman, Phys. Rev. A **86**, 063639 (2012).

[30] V. Galitski and I. B. Spielman, Nature **494**, 49 (2013).

[31] L. Tonks, Phys. Rev. **50**, 955 (1936).

[32] M. Girardeau, J. Math. Phys. **1**, 516 (1960).

[33] E. H. Lieb, W. Liniger, Phys. Rev. **130**, 1605 (1963).

[34] C. N. Yang, Phys. Rev. Lett. **19**, 1312 (1967).

[35] M. Gaudin, Phys. Lett. A **24**, 55 (1967).

[36] J. K. Jain, Phys. Rev. Lett. **63**, 199 (1989).

[37] A. Lopez and E. Fradkin, Phys. Rev. B **44**, 5246 (1991).

[38] B. Halperin, P. A. Lee and N. Read, Phys. Rev. B **47**, 7312 (1993).

[39] R. Shankar, Ann. Phys. (Berlin) **523**, 751 (2011).

[40] T. S. Jackson, N. Read, and S. H. Simon, arXiv:1303.4716.

[41] F. D. M. Haldane, Phys. Rev. Lett. **61**, 2015 (1988).

[42] Note that the semiclassical expression (2) is exact only for small $\nu_l \ll 1$. For $\nu_0 \approx 1/2$ it is only approximate.

[43] H. F. Baker, Proc. London Math. Soc (2) 3, 24 (1905); J. E. Campbell, Proc. London Math. Soc. (1) 28, 381 (1897), 29, 14 (1897); S. F. Hausdorff, Leipz. Ber. 58, 19 (1906).

[44] C. Kittel, *Introduction to Solid State Physics*, Wiley, New York (2005).

[45] M.V. Berry, Proc. R. Soc. Lond. A **392**, 45 (1984).

[46] J. N. Fuchs, F. Piechon, M.O. Goerbig, and G. Montambaux, Eur. Phys. J. B **77**, 351 (2010).

[47] D. R. Hofstadter, Phys. Rev. B **14**, 2239 (1976).

[48] S. Katsura, T. Ide, and T. Morita, J. of Stat. Phys., **42**, 381 (1986).

[49] J. B. Fouet, P. Sindzingre, and C. Lhuillier, Eur. Phys. J. B **20**, 241 (2001).

[50] C. N. Varney, K. Sun, M. Rigol, and V. Galitski, Phys. Rev. B **82**, 115125 (2010).

[51] C. N. Varney, K. Sun, V. Galitski and M. Rigol, New J. of Phys. **14**, 115028 (2012).